Chapter

Raman Spectroscopy of Graphene, Graphite and Graphene Nanoplatelets

Daniel Casimir, Hawazin Alghamdi, Iman Y. Ahmed, Raul Garcia-Sanchez and Prabhakar Misra

Abstract

The theoretical simplicity of sp^2 carbons, owing to their having a single atomic type per unit cell, makes these materials excellent candidates in quantum chemical descriptions of vibrational and electronic energy levels. Theoretical discoveries, associated with sp^2 carbons, such as the Kohn anomaly, electron-phonon interactions, and other exciton-related effects, may be transferred to other potential 2D materials. The information derived from the unique Raman bands from a single layer of carbon atoms also helps in understanding the new physics associated with this material, as well as other two-dimensional materials. The following chapter describes our studies of the G, D, and G′ bands of graphene and graphite, and the characteristic information provided by each material. The G-band peak located at ~1586 cm^{-1}, common to all sp^2 carbons, has been used extensively by us in the estimation of thermal conductivity and thermal expansion characteristics of the sp^2 nanocarbon associated with single walled carbon nanotubes (SWCNT). Scanning electron microscope (SEM) images of functionalized graphene nanoplatelet aggregates doped with argon (A), carboxyl (B), oxygen (C), ammonia (D), fluorocarbon (E), and nitrogen (F), have also been recorded and analyzed using the Gwyddion software.

Keywords: Raman spectroscopy, 2-D materials, graphene, graphite, functionalized graphene nanoplatelets

1. Introduction

The elucidation of novel physics related to 2D electronic systems (2DES) has received wide recognition in the form of three Nobel Prizes in Physics in 1985 [1] (Klaus von Klitzing, Max Planck Institute, for the discovery of the integer Quantum Hall Effect), in 1998 [2] (Robert Laughlin, Stanford University, Horst Stormer, Columbia University, and Daniel Tsui, Princeton University, for the discovery of the fractional Quantum Hall Effect), and in 2010 [3] (Andre Geim and Konstantin Novoselov, University of Manchester, for ground-breaking experiments relating to the 2D material graphene).

Since graphene can be considered as the conceptual parent material for all other sp^2 nanocarbons, it is the first in our discussion of the two-dimensional characteristics obtainable via Raman spectroscopy. Graphene is a two-dimensional carbon

nanomaterial with a single layer of sp^2-hybridized carbon atoms arranged in a crystalline structure of six-membered rings [4, 5]. **Figure 1** illustrates the hexagonal lattice of a perfectly flat graphene sheet and the resulting nanotube after it is rolled along the vector labeled $\mathbf{C_h}$. The shaded portion of the nanotube in **Figure 1(b)** represents one unit cell of the resulting armchair nanotube in this case, and it results from rolling the initial planar sheet in **Figure 1(a)**, so that points **A** and **C** coincide with points **B** and **D**, respectively. $\mathbf{C_h}$ is known as the chiral vector and is constructed from the vector addition of the graphene basis vectors $\mathbf{a_1}$ and $\mathbf{a_2}$. The integer number of each of the basic lattice vectors used in the construction, n and m, designated for $\mathbf{a_1}$ and $\mathbf{a_2}$ respectively, is arbitrary with the only provision that $(0 \leq |m| \leq n)$. The Cartesian components of the lattice vectors $\mathbf{a_1}$ and $\mathbf{a_2}$ are $(a\sqrt{3}/2, a/2)$ and $(a\sqrt{3}/2, -a/2)$, respectively, where the quantity $a = a_{C\text{-}C}\sqrt{3} = 2.46$ Å. The quantity $a_{C\text{-}C}$ is the bond length between two neighboring carbon atoms in the hexagonal lattice equal to 1.42 Å. The chiral vector $\mathbf{C_h}$ is usually written in terms of the two integers n and m as

$$\mathbf{C_h} = n\,\mathbf{a_1} + m\,\mathbf{a_2} \tag{1}$$

and has a magnitude of

$$|\mathbf{C_h}| = a\sqrt{n^2 + m^2 + nm} \tag{2}$$

which equals the carbon nanotube's circumference. In a fashion similar to applying the above rolling operation on the graphene unit cell in **Figure 1** for the construction of single walled carbon nanotubes, graphite can be described in terms of stacking multiple graphene layers one atop the other.

We have also investigated functionalized graphene nanoplatelets, which are comprised of platelet-shaped graphene sheets, identical to those found in SWCNT, but in planar form. Among the samples we used (functionalized oxygen, nitrogen, argon, ammonia, carboxyl and fluorocarbon) all have similar shape. Graphene nanoplatelet aggregates (aggregates of sub-micron platelets with a diameter of <2 μm and a thickness of a few nanometers) were identified, rather than individual nanoplatelets (STREM Data Sheets [6]). According to the manufacturer's (Graphene Supermarket™), structural analysis for fluorinated graphene nanoplatelets (GNP), the lateral dimensions of the wrinkled sheet-like outer surface of the GNP's is ~1–5 μm [6]. The quoted number of graphene layers was also around 37

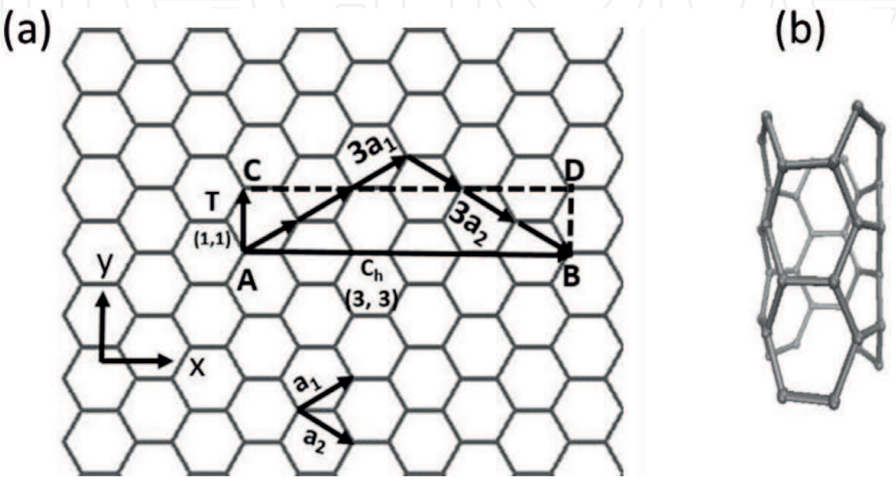

Figure 1.
(a) Construction of a carbon nanotube based on the lattice vectors of a planar hexagonal graphene sheet. (b) The resulting armchair (3, 3) carbon nanotube.

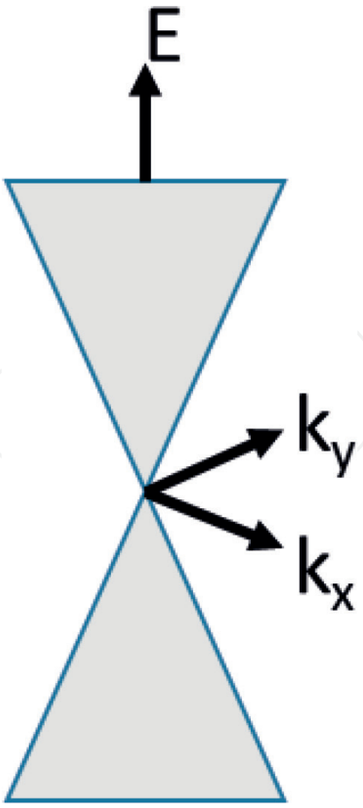

Figure 2.
The linear E vs. k dispersion of graphene near the Brillouin zone K-point (Dirac cone).

layers, based on SEM and TEM analysis [7]. This average number of layers is more than sufficient to consider these sub-micron sized stacked graphene nanoparticles as being in the multi-layer graphene category, and not in the few layer category. This latter property of GNP's is also mentioned in the concluding remarks, in connection with their two-dimensional classification.

Arguably one of the most striking displays of the two-dimensional nature of graphene is related to its electronic structure; specifically, the behavior of its electron/hole carriers [4]. The resulting dispersion (E vs. **k**) relation of the graphene band structure forces us to rely on Dirac's relativistic wave equation, instead of Schrodinger's equation, to describe the particle dynamics [4]. Therefore, the charge carriers are treated as relativistic massless quantities moving essentially at the speed of light [4].

Figure 2 shows one of the six "Dirac cones," which are one of the highly symmetrized K point locations in graphene's Brillouin zone, as shown in **Figure 3**, where the valence and conduction bands touch one another [4]. The experimental verification of this linear dispersion for energies centered at and near the Dirac cone as expressed in Eq. (3) has also been accomplished by various spectroscopic methods [8].

$$E\left(\vec{k}\right)^{\pm} = \pm\hbar v_F\left|\vec{k}\right| \tag{3}$$

Another significant electronic structural quantity that expresses the two-dimensional nature of graphene is the density of states (DOS), g**(E)**, which as its name suggests, gives the density of mobile charge carriers that are available at some temperature T [4]. Unsurprisingly, this quantity also varies linearly, only this time with the energy E, as expressed in Eq. (4) [4].

$$\boldsymbol{g(E)} = \frac{2}{\pi\left(\hbar v_F\right)^2}|\boldsymbol{E}| \tag{4}$$

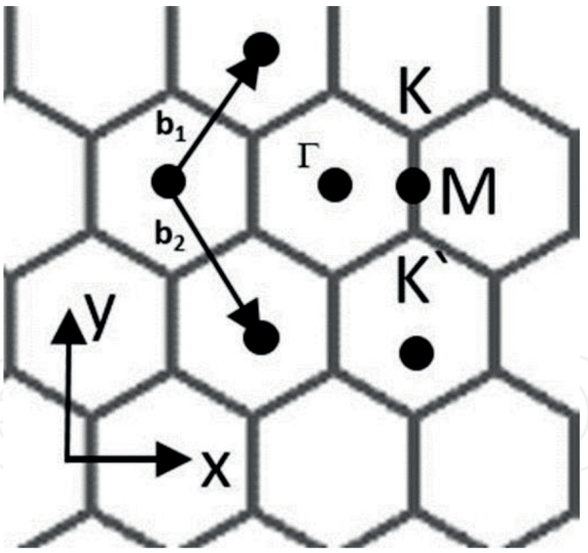

Figure 3.
Graphene's reciprocal space lattice shown with reciprocal lattice vectors b1, and b2. The first Brillouin zone is the region labeled by Γ. Also shown are the six high symmetry regions, Γ, K, M, and K'.

The 2D nature of graphene plays a direct role in this result, sine g(E), which gives the number of available states within the energy interval E and E + dE, is defined in two-dimensions in terms of the ratio of an element of area dA in k-space per unit wave-vector k.

2. Experimental

Figure 4 shows the primary instrument used to record most of the Raman spectra; it was a DXR SmartRaman spectrometer from Thermoelectron (that uses 780, 532, and 455 nm laser sources). The first wavelength (780 nm) was used for the bulk of the recorded spectra and utilized a high brightness laser of the single mode diode (as does the 532 nm light source), while the 455 nm source is a diode-pumped solid-state laser. Using the 180° geometry, after focusing the laser beam on the sample, the backscattered radiation from the sample enters the spectrometer via a collection lens, and the Stokes-shifted Raman spectrum was recorded as read by the CCD detector using the correct Rayleigh filter and automated entrance slit selections. A full range grating was used with the triplet spectrograph.

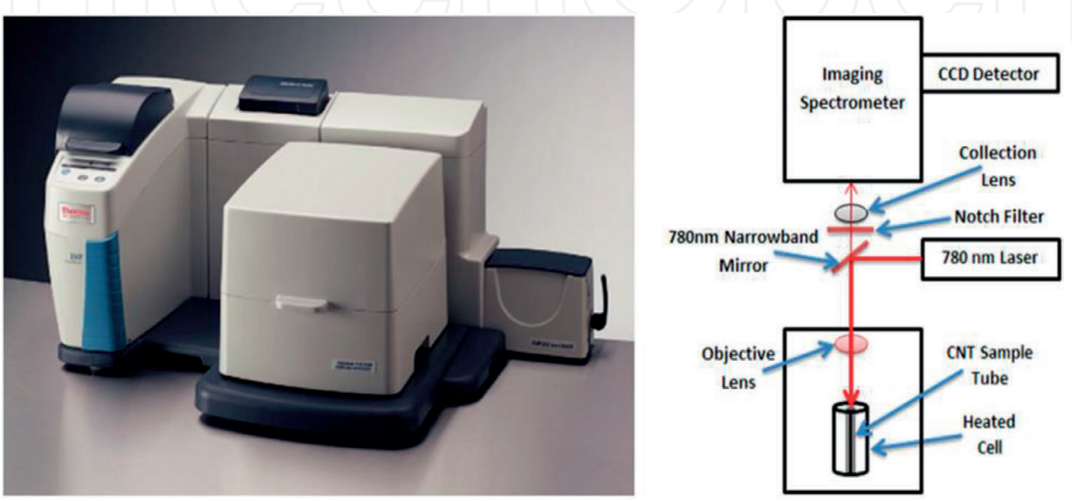

Figure 4.
DXR SmartRaman spectrometer (left) and DXR schematic (right).

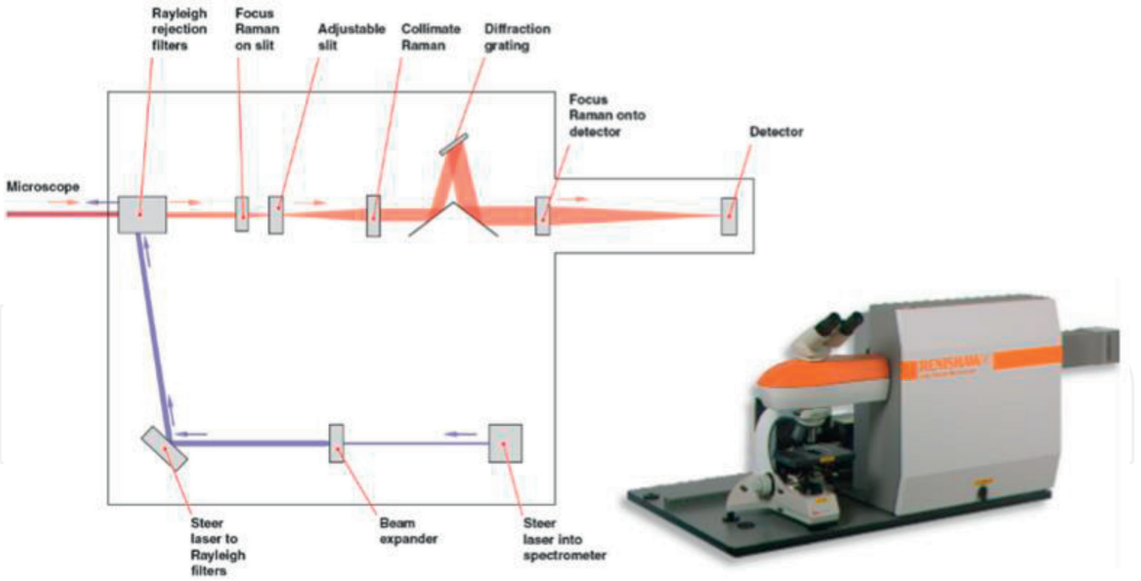

Figure 5.
InVia Raman spectrometer schematic and instrument image from the Renishaw manual.

Figure 6.
Two views of the JEOL JSM-7600F scanning electron microscope (SEM) setup.

The Renishaw inVia Raman spectrometer (**Figure 5**) uses a 532-nm laser source and was employed to record the Raman spectra of CVD graphene and the functionalized graphene nanoplatelets. It consists of a microscope to shine light on the sample and collecting the scattered light, after filtering all the light except for the tiny fraction that has been Raman scattered, together with a diffraction grating for splitting the Raman scattered light into its component wavelengths, and a CCD camera for final detection of the Raman spectrum.

Graphene nanoplatelets (GNP) are usually produced by the intercalation of graphite through various means, followed by an acid purification process, and further exfoliation of the initial GNP flakes [9]. Besides intercalation, irradiation with microwaves, or extreme heating is also sometimes used to produce GNP from the host graphite source [10].

Images of functionalized graphene nanoplatelets were taken with the JEOL JSM-7600F scanning electron microscope (SEM) shown in **Figure 6**. The secondary electron detector on the SEM uses an EMI current of 138.20 nA. Beam current employed had a range of 1 pA to 200 nA. The JEOL JSM-7600F SEM contains a large variety of detectors that can be used on specimen samples up to 200 mm in diameter. Various magnifications were selected when appropriate to accurately

display sample structure; SEM magnification ranges between 25 and 1,000,000×. The modular software program Gwyddion was used to generate three-dimensional visualization of the nanoplatelet aggregate structures.

3. Results

The structural simplicity of graphene is also exhibited in its Raman spectrum in contrast to its other fullerene relatives [11]. The two prominent bands located at 1580 and 2700 cm^{-1} are customarily called the G and G′-bands, respectively [11]. The high energy first order G-band has been identified with the intra-planar stretching modes of the strongly connected σ-bonded carbons [5]. The G′-band at 2700 cm^{-1} is attributed to a second order Raman scattering event with the phonon wave vector $q \neq 0$ [5]. **Figure 7** shows both bands obtained from a graphene sample on a nickel substrate.

Discerning the two-dimensional nature of graphene can be accomplished by contrasting the G′-band features of graphite and the former material [11]. First, the relative intensities between the G and G′ bands are different for graphene and its macroscopic relative graphite. In the case of graphene, the G′-band has a greater intensity than the G-band, which is the case for G-bands illustrated in **Figures 7** and **8**. The G′-band of graphite is also shifted to a higher frequency compared to that of graphene [11]. Thirdly, the overall shape of the G′-band is usually more uniform compared to that of graphite, usually requiring a single Lorentzian to be fitted [11]. This last effect especially arises due to interactions among the multiple layers of graphite [11]. The Raman spectrum of the graphene sample was recently collected on an aged sample, and the degradation and contamination of this extremely thin material over time may be responsible for our Raman spectra of graphene and graphite only satisfying the first of these three criteria convincingly.

Not only the dimensionality, or number of layers present can be obtained via the Raman bands of graphene or graphite, but the average lateral characteristic size can of the graphene layers in the beam spot can also be determined. This was initially

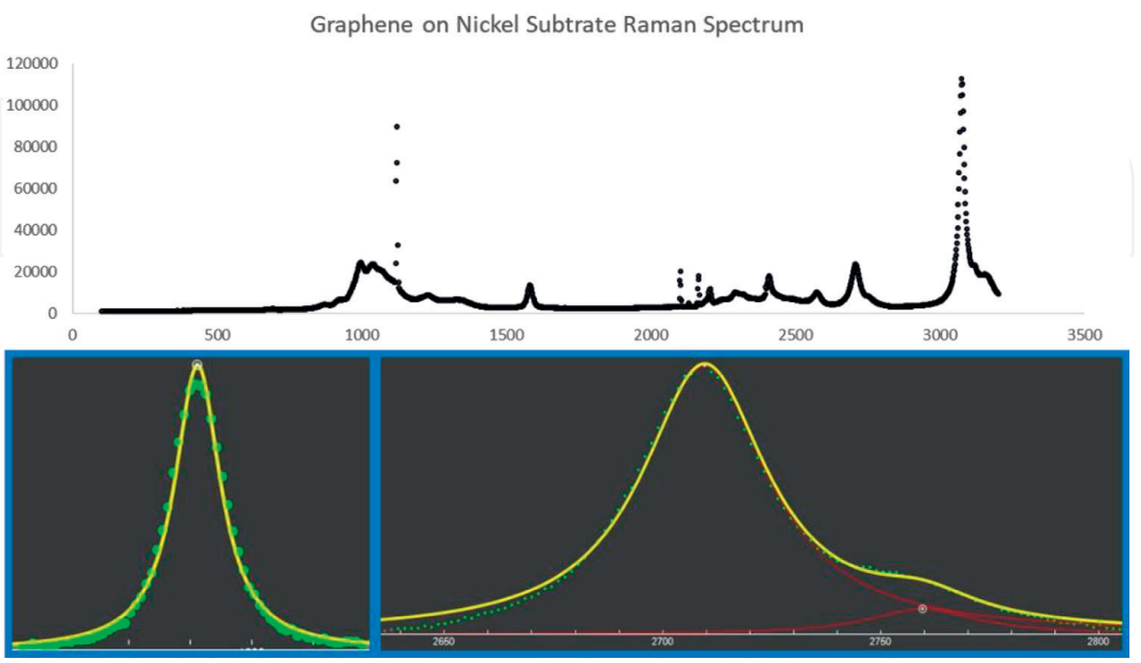

Figure 7.
(Top) Raman spectrum of CVD graphene on nickel substrate collected using 514 nm laser excitation. (Bottom left) G-band and Lorentzian (1582.4 cm^{-1}, height: 11,655.9). (Bottom right) G'-band and Lorentzians (2709.6 cm^{-1}, 2759.6 cm^{-1}, heights: 19,669.9, 1856.6).

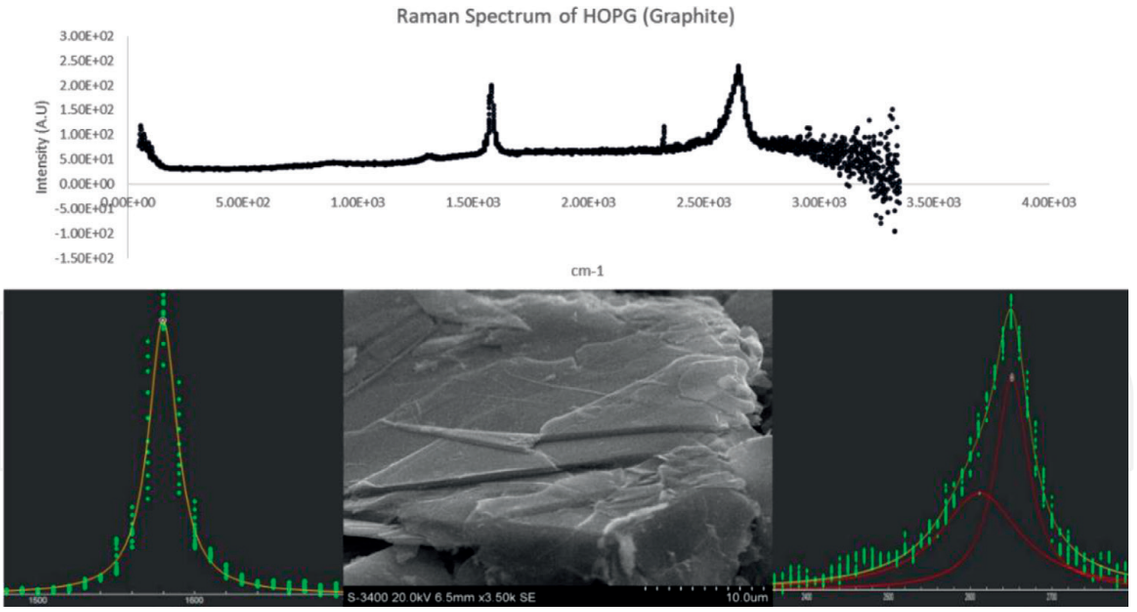

Figure 8.
(Top) Raman spectrum of HOPG graphite at excitation of 780 nm. (Bottom left) G-band and Lorentzian (1579.7 cm^{-1}, height: 128.9); (Bottom middle) SEM image of HOPG sample; (Bottom right) G'-band and Lorentzians (2611.8 cm^{-1}, 2651 cm^{-1}, heights: 56.1, 123.1).

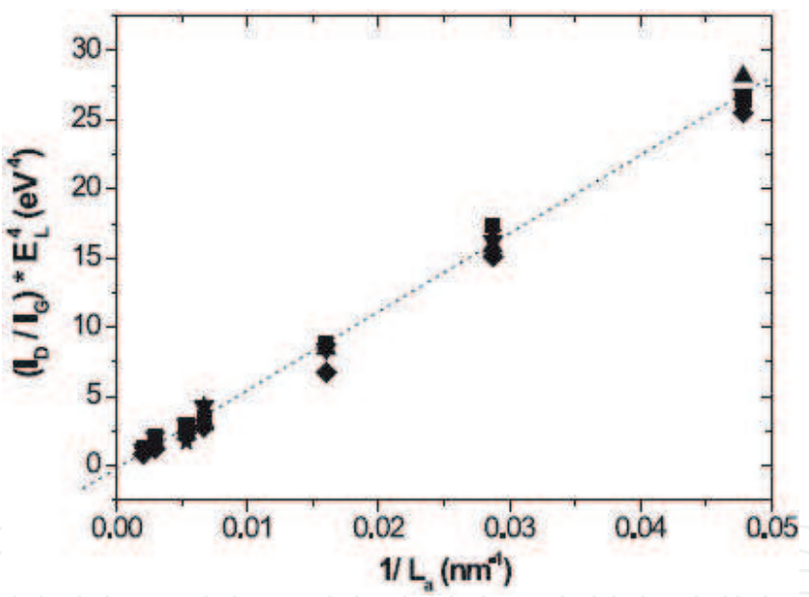

Figure 9.
Plot of $(I_D/I_G)*(E_L)^4$ vs. $1/L_a$. E_L is the laser excitation energy in eV, I_D and I_G are the D and G band intensities, respectively, and L_a is the characteristic lateral size of the graphene layer. Adapted from [5].

discovered by Tuinstra and Koenig, who correctly deduced that the intensity ratio of the D and G-bands varies directly with the characteristic size La of the planar graphite crystallites [12]. Further work done by Cancado et al. [13], expanded on Tuinstra and Koenig's work, by demonstrating the excitation energy dependence of the proportionality factor in the original relation as shown in **Figure 9** and as expressed in Eq. (5).

$$L_a = \left(2.4 \times 10^{-10}\right) \lambda^4 \left(\frac{I_D}{I_G}\right)^{-1} \quad (5)$$

For the graphene sample in **Figure 7** with a D-band intensity of 2719.7 and the graphite sample in **Figure 8** with a D-band intensity of 8.6, the respective L_a values are 71.8 nm and 1.3 μm according to Eq. (5) (**Table 1**).

Element	*x* average (μm)	*y* average (μm)	*z* average (μm)
Argon	4.8	3.9	0.50
Carboxyl	4.3	4.5	0.57
Oxygen	4.7	4.3	0.90
Ammonia	4.4	3.7	0.64
Fluorocarbon	5.0	3.6	0.55
Nitrogen	6.7	6.5	0.91

Table 1.
Average x, y, z axis measurements of functionalized graphene nanoplatelet aggregates.

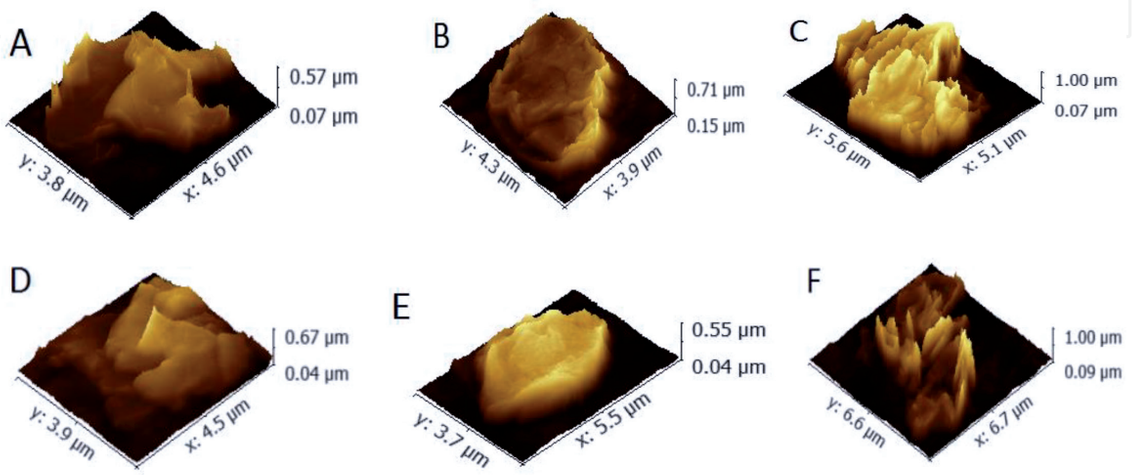

Figure 10.
3D view of SEM data of functionalized graphene nanoplatelet aggregates doped with argon (A), carboxyl (B), oxygen (C), ammonia (D), fluorocarbon (E), and nitrogen (F), respectively, using Gwyddion software.

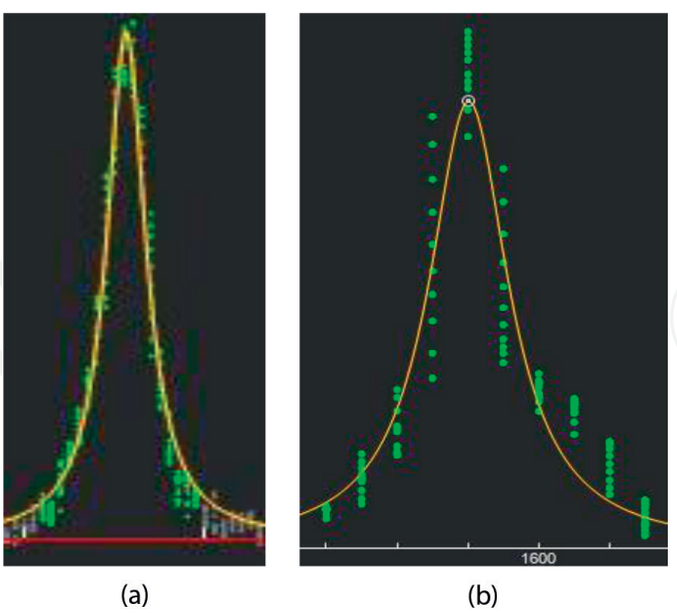

Figure 11.
(a) D-band on left (Intensity: 33.5, Center: 1312.4 cm^{-1}), (b) G-band on right (Intensity: 62.5, Center: 1580.2 cm^{-1}) for graphene nanoplatelets (ammonia) with 780 nm excitation and using fityk peak fitting software [14].

The observed sub-micron size of the platelets obtained mentioned above, and imaged in **Figure 10**, was also verified via Raman spectroscopy, based on the use of Eq. (3) for the graphene nanoplatelets functionalized with Ammonia, whose D and G bands are shown in **Figure 11**.

For an excitation wavelength of 780 nm, the characteristic size L_a, for this sample calculates to a value of 0.17 μm. This characteristic sheet size corresponds with the dimensions for the aggregate samples shown in **Figure 10**. This value is also closer in magnitude to the calculated L_a value for graphite, than that for graphene, due to the greater chance for multiple stacked sheets among the graphene nanoplatelets to be responsive to the measurements.

4. Conclusion

To recap, in this chapter we have discussed the ability to discern whether certain graphitic nanomaterials are primarily 2 or 3 dimensional in character, based on features of their Raman bands. For all three materials (namely graphene, graphite, and functionalized graphene nanoplatelets), we have made use of Tuinstra and Koenig's relationship between the intensities of the D and G Raman bands to characterize the nanomaterials. In addition to the analysis based on Raman spectroscopy, SEM visualization/dimensional analysis was also performed on the graphene nanoplatelet samples. To conclude, the bulk macroscopic 3D character of graphite was clearly apparent compared to the 2D nature of graphene. However, based on the results for the graphene nanoplatelets, both 2D and 3D characteristics/behaviors were present for them, without one dimension dominating the other.

Acknowledgements

Financial support from the National Science Foundation (Award# PHY-1358727 and PHY-1659224) is gratefully acknowledged.

Conflict of interest

No conflict of interest.

Author details

Daniel Casimir, Hawazin Alghamdi, Iman Y. Ahmed, Raul Garcia-Sanchez and Prabhakar Misra*
Laser Spectroscopy Laboratory, Howard University, Washington, DC, USA

*Address all correspondence to: pmisra@howard.edu

References

[1] Nobelprize.org Physics Prize (1985) [Internet]. 2018. Available from: https://www.nobelprize.org/prizes/physics/1985/summary

[2] Nobelprize.org Physics Prize (1998) [Internet]. 2018. Available from: https://www.nobelprize.org/prizes/physics/1998/summary

[3] Nobelprize.org Physics Prize (2010) [Internet]. 2018. Available from: https://www.nobelprize.org/prizes/physics/2010/press-release

[4] Wong HSP, Akinwande D. Carbon Nanotube and Graphene Device Physics. New York: Cambridge University Press; 2011

[5] Jorio A, Saito R, Dresselhaus G, Dresselhaus M. Raman Spectroscopy in Graphene Related Systems. Weinheim: Wiley-VCH Verlag GmbH & Co. KGaA; 2011

[6] STREM Graphene Nanoplatelets Data Sheet [Internet]. Available from: https://secure.strem.com/uploads/resources/documents/graphene_nanoplatelets_copy1.pdf

[7] Graphene Supermarket Fluorinated Graphene Nanoplatelets Data [Internet]. Available from: https://graphene-supermarket.com/Fluorinated-Graphene-Nanoplatelets.html

[8] Binning G, Rohrer H, Gerber C, Weibel E. Surface studies by scanning tunneling microscopy. Physical Review Letters. 1982;**49**:57

[9] Chieng WB, Ibrahim NA, Yunus WMZW, Hussein MZ, Then YY, Loo YY. Effects of graphene nanoplatelets and reduced graphene oxide on poly(lactic acid) and plasticized poly (lactic acid): A comparative study. Polymers. 2014;**6**:2232-2246

[10] Cunha E, Ren H, Lin F, Kinloch IA, Sun Q, Fan Z, et al. The chemical functionalization of graphene nanoplatelets through solvent-free reaction. Royal Society of Chemistry Advances. 2018;**8**:33564-33572

[11] Hodkiewicz J. Characterizing carbon materials with Raman spectroscopy. Thermo-Fisher Scientific Application Note. 2010;**51901**:1-5

[12] Tuinstra F, Koenig JL. Raman spectrum of graphite. The Journal of Chemical Physics. 1970;**53**(3):1126-1130

[13] Cancado LG, Takai K, Enoki T, Endo M, Kim YA, Mizuasaki H, et al. Measuring the degree of stacking order in graphite by Raman spectroscopy. Carbon. 2008;**46**:272-275

[14] Wojdyr M. Fityk a general-purpose peak fitting program. Journal of Applied Crystallography. 2010;**43**:1126-1128